Electronic Supplementary Material (ESI) for Journal of Materials Chemistry A.

Active Fe_2O_3 nanoparticles encapsulated in porous g-C_3N_4/graphene sandwich-type nanosheets as superior anode for high-performance lithium-ion batteries

Minjie Shi, Tianhao Wu, Xuefeng Song,* Jing Liu, Liping Zhao, Peng Zhang, Lian Gao*

State Key Laboratory for Metallic Matrix Composite Materials,
School of Materials Science and Engineering,
Shanghai Jiao Tong University, Shanghai 200240, P. R. China
*E-mail: liangao@mail.sic.ac.cn (L. Gao); songxfeng@sjtu.edu.cn (X. F. Song)

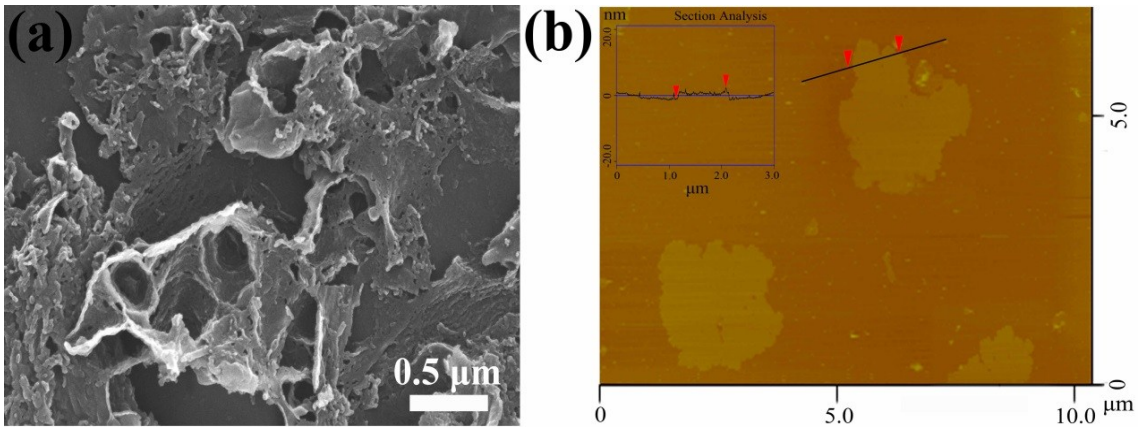

Fig. S1. (a) FESEM and (b) AFM images of ultrathin g-C_3N_4 nanosheets.

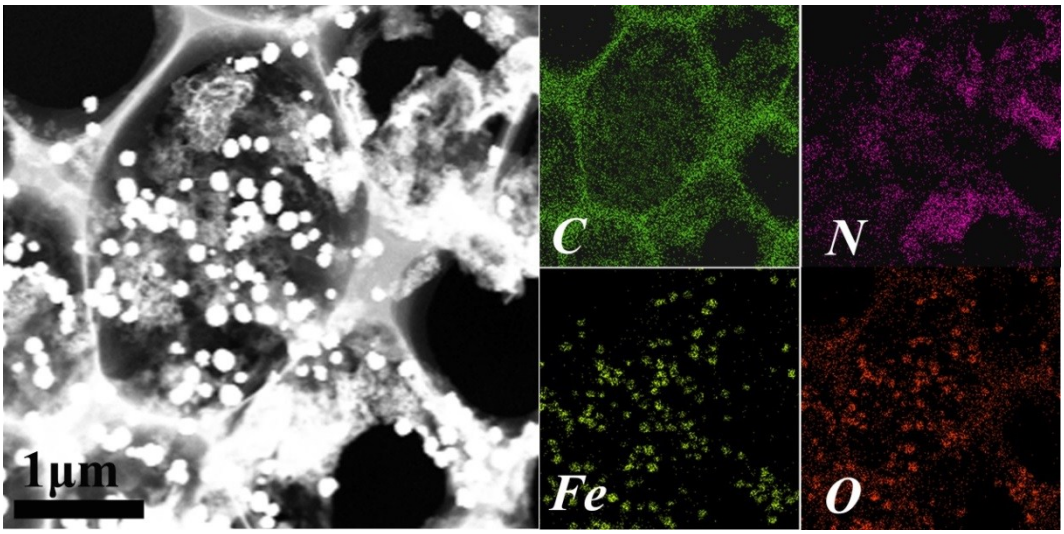

Fig. S2. (a) Scanning transmission electron microscopy image of Fe_2O_3/CN-G composite and corresponding elemental mapping images.

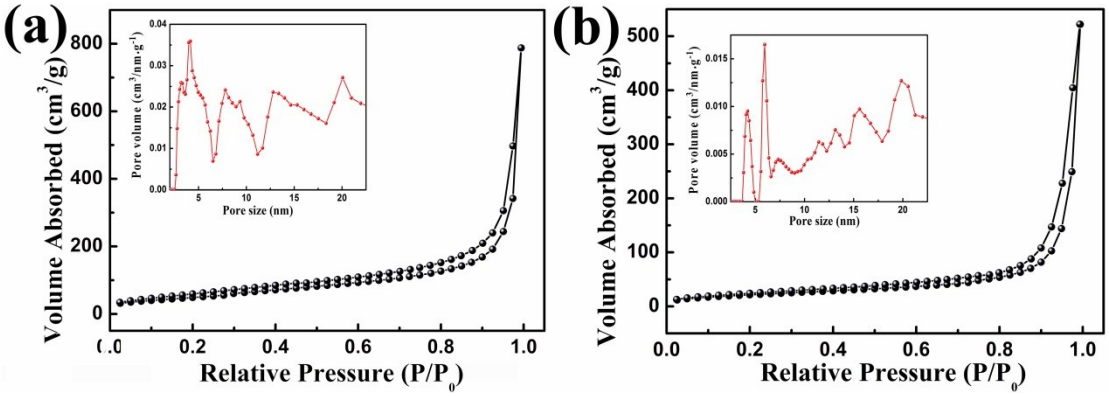

Fig. S3. (a) Nitrogen adsorption/desorption isotherm and pore size distribution curve of g-C_3N_4. The specific surface area of the ultrathin g-C_3N_4 is as high as 211.4 m^2/g, while abundant mesoporous is ranging from 2 to 20 nm. (b) Nitrogen adsorption/desorption isotherm and pore size distribution curve of Fe_2O_3/CN-G composite. The Fe_2O_3/CN-G has a specific surface area of 81.22 m^2/g and represents mesopore size distribution concentrated at about 4~6 nm.

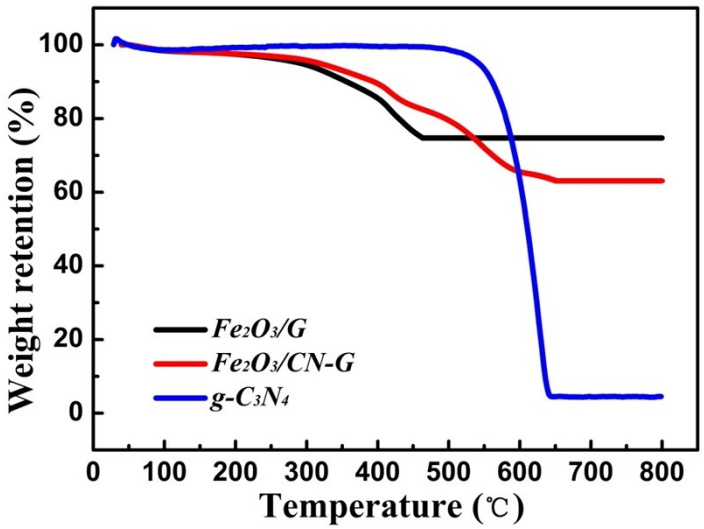

Fig. S4. TGA curves of g-C_3N_4, Fe_2O_3/G and Fe_2O_3/CN-G ranging from 50 to 800 °C at a heating rate of 10°C /min under air flow. As seen from the TGA curve (red) of Fe_2O_3/CN-G, there are two major weight loss in the whole temperature range: the first one appeared between 150 °C and 460 °C is resulted from the decomposition of graphene; the second one appeared between 480 °C and 650 °C is attributed to the pyrolysis of g-C_3N_4, so the calculated mass content of graphene and g-C_3N_4 in Fe_2O_3/CN-G composite is 18.8 wt% and 19.7 wt%, respectively.

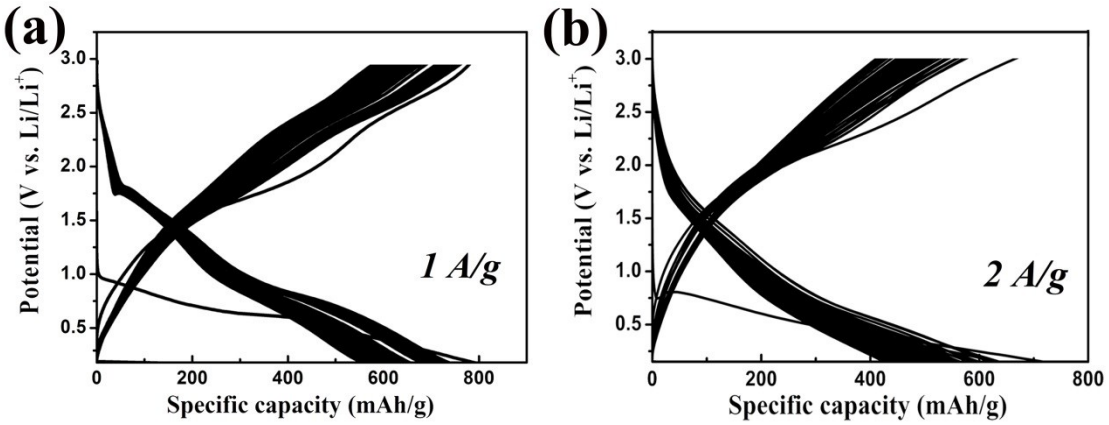

Fig. S5 Galvanostatic charge/discharge curves of Fe_2O_3/CN-G for 100 cycles at current density of (a) 1 A/g and (b) 2 A/g, respectively.

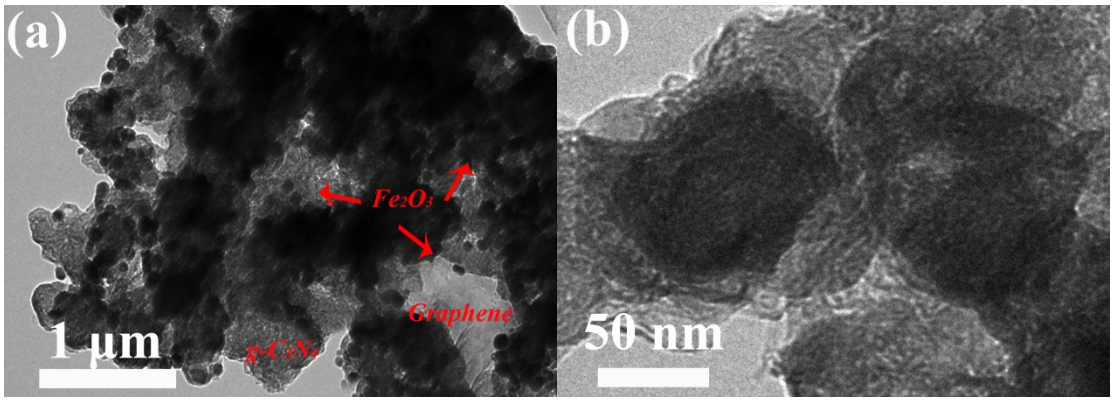

Fig. S6 TEM images of Fe_2O_3/CN-G electrode after 50 cycles at 50 mAh/g in LIBs.

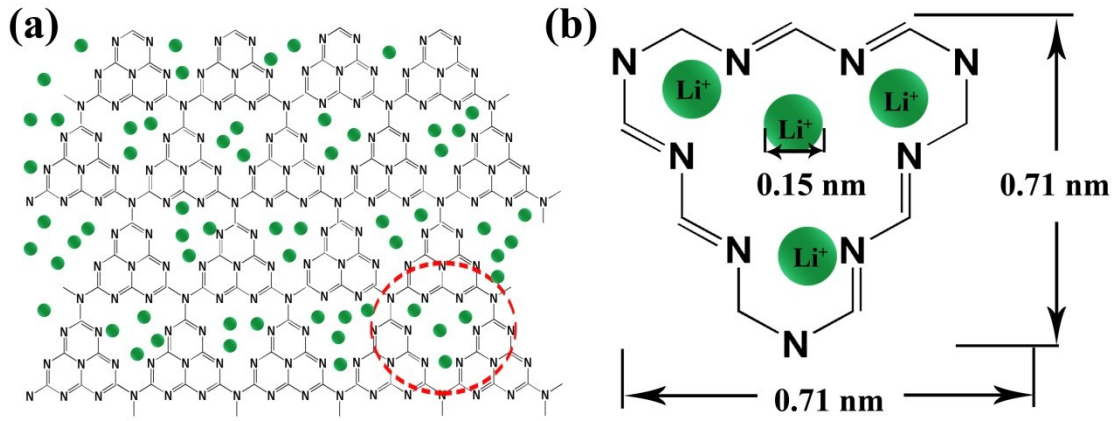

Fig. S7. (a) Schematic model of g-C_3N_4 with plentiful triangular void spaces for dispersed decoration and absorption of Li^+ ions druing the electrochemical process. (b) Structure magnification of the triangular space with the appropriate size in g-C_3N_4, which offer sufficient accommodation for Li^+ with electron charge, thereby further increase the reversible capacity.

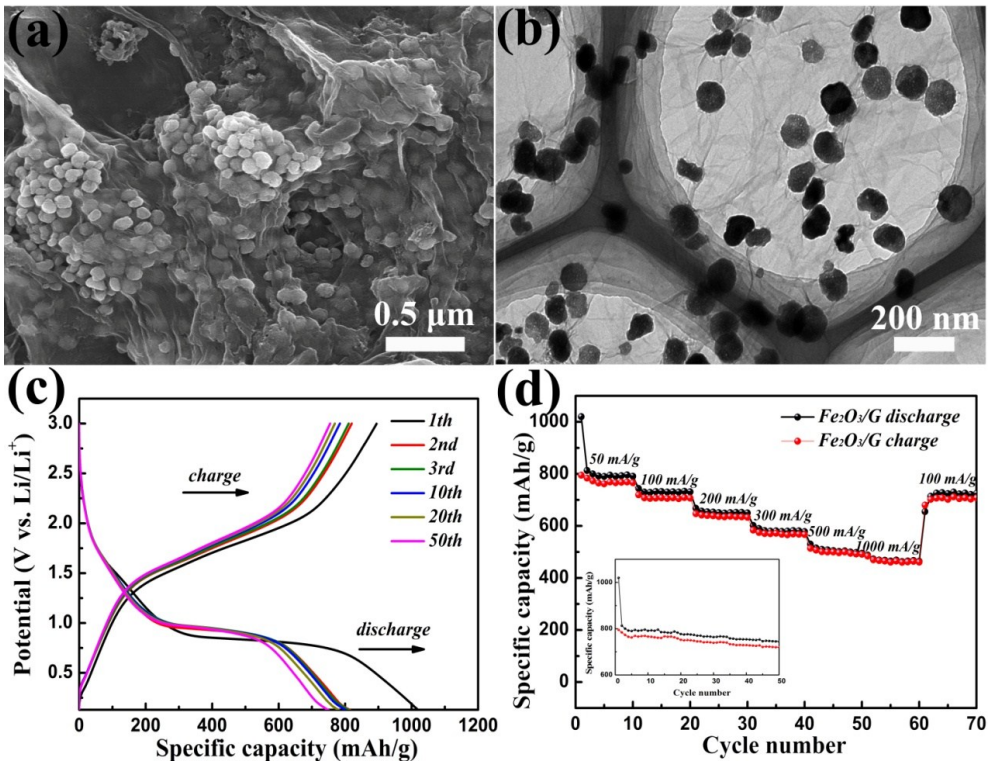

Fig. S8. (a) FESEM and (b) TEM images of Fe_2O_3/G. (c) Galvanostatic charge/discharge profiles for 50 cycles at a current density of 50 mA/g and (d) rate capability and cycling performance (inset) of Fe_2O_3/G. The Fe_2O_3/G agglomerate with each other to form multilayer structure owing to the natural tendency to the restacking of graphene, which could reduce the active surface area and slow down the transfer of charge and Li^+ ions between electrolyte and bulk electrode, thereby leading to the unsatisfactory electrochemcial performance compared with Fe_2O_3/CN-G.

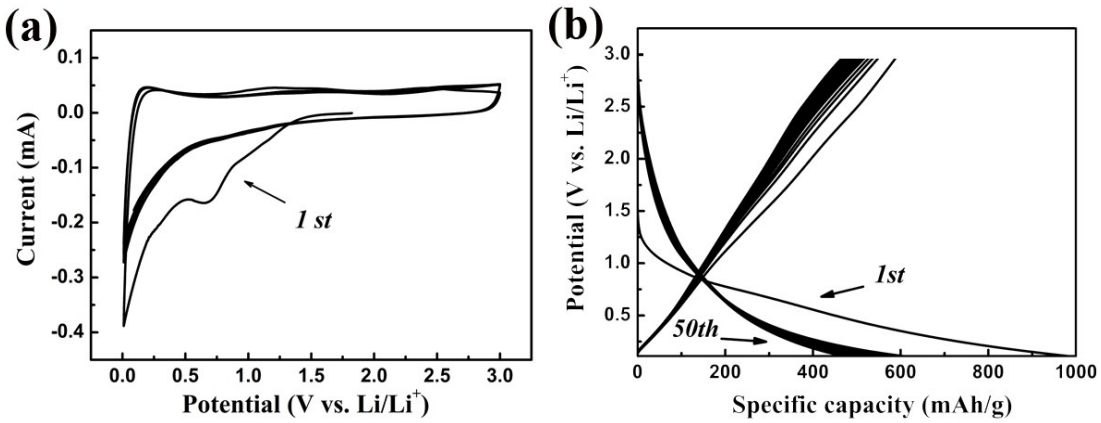

Fig. S9. Cyclic voltammetry curve of g-C_3N_4-Graphene anode in the initial five cycles at a scan rate of 0.1 mV/s. (b) Galvanostatic charge/discharge profiles of g-C_3N_4-Graphene in 50 cycles at a current density of 50 mA/g. The g-C_3N_4-Graphene anode can delivers a reversible capacity of 586 mAh/g after 5 cycles and 462 mAh/g after 50 cycles.

Table S1. Representative rate capability and cycle stability ever reported for state-of-the-art metal oxide/graphene anode materials in LIBs for comparison with our results.

Anode material	Rate capability	Capacity performance after cycling	Ref.
SnO_2/G	622 mAh/g at 0.78 A/g	508 mAh/g (at 78 mA/g) after 50 cycles	1
NiO_2/G	245 mAh/g at 1 A/g	700 mAh/g (at 100 mA/g) after 50 cycles	2
Co_3O_4/G	~560 mAh/g at 0.5 A/g	767 mAh/g (at 50 mA/g) after 50 cycles	3
Mn_3O_4/G	~600 mAh/g at 0.8 A/g	~730 mAh/g (at 400 mA/g) after 40 cycles	4
Fe_3O_4/G	~600 mAh/g at 1.05 A/g	950 mAh/g (at 35 mA/g) after 85 cycles	5
Fe_2O_3/G	N/A	742 mAh/g (at 100 mA/g) after 50 cycles	6
Fe_2O_3/G	~580 mAh/g at 0.8 A/g	~745 mAh/g (at 100 mA/g) after 100 cycles	7
Fe_2O_3/G	~512 mAh/g at 0.8 A/g	660 mAh/g (at 50 mA/g) after 100 cycles	8
Fe_2O_3/CN-G	730 mAh/g at 1 A/g	980 mAh/g (at 50 mA/g) after 50 cycles	Our results

Notes and references

1. S. Yang, W. B. Yue, J. Zhu, Y. Ren and X. J. Yang, *Advanced Functional Materials*, 2013, **23**, 3570.
2. D. F. Qiu, Z. J. Xu, M. B. Zheng, B. Zhao, L. J. Pan, L. Pu and Y. Shi, *Journal of Solid State Electrochemistry*, 2012, **16**, 1889.
3. Z. S. Wu, W. C. Ren, L. Wen, L. B. Gao, J. P. Zhao, Z. P. Chen, G. M. Zhou, F. Li and H. M. Cheng, *ACS Nano*, 2010, **4**, 3187.
4. H. L. Wang, L. F. Cui, Y. A. Yang, H. S. Casalongue, J. T. Robinson, Y. Y. Liang, Y. Cui and H. J. Dai, *Journal of the American Chemical Society*, 2010, **132**, 13978.
5. G. M. Zhou, D. W. Wang, F. Li, L. L. Zhang, N. Li, Z. S. Wu, L. Wen, G. Q. Lu and H. M. Cheng, *Chemistry of Materials*, 2010, **22**, 5306.
6. D. Z. Chen, W. Wei, R. N. Wang, J. C. Zhu and L. Guo, *New Journal of Chemistry*, 2012, **36**, 1589.
7. X. J. Zhu, Y. W. Zhu, S. Murali, M. D. Stollers and R. S. Ruoff, *ACS Nano*, 2011, **5**, 3333.
8. G. Wang, T. Liu, Y. J. Luo, Y. Zhao, Z. Y. Ren, J. B. Bai and H. Wang, *Journal of Alloys and Compounds*, 2011, **509**, L216.